Lithographic Simulation: A Review

Chris A. Mack
KLA-Tencor, FINLE Division
Suite 301, 8834 N. Capital of Texas Highway, Austin, TX 78759

Abstract

A review of the current state of the art in optical and electron beam lithography simulation is presented. Basic physical models are described and examples are given. In addition, rigorous electromagnetic simulation for mask topography is shown and the use of statistical modeling to predict feature size distributions in manufacturing is described. Finally, numerous examples of the use of lithography simulation and its impact on the semiconductor industry are offered.

Keywords: Lithography Simulation, Optical Lithography, Electron Beam Lithography, Electromagnetic Field Simulation, PROLITH, ProBEAM/3D, ProMAX/2D, ProCD

1. Introduction

Optical and electron beam lithographies are the mainstay of patterning techniques for semiconductor manufacturing. Electron beam lithography, in either raster or vector scan forms, remains critical for the manufacture of advanced photomasks. These photomasks, in turn, are used in optical projection step and repeat or step and scan cameras for the mass production of integrated circuits with feature sizes down to 100nm. To aid in the development, optimization, and use of the equipment, materials, and processes for these lithographic technologies, simulation has become a widely used tool. Fortunately, the same technologies developed for semiconductor lithography simulation can be applied to wide range of lithographic applications. This paper will present a review of the current state of the art in optical and electron beam lithography simulation. Basic physical models are described and examples are given. In addition, rigorous electromagnetic simulation for mask topography is shown and the use of statistical modeling to predict feature size distributions in manufacturing is described. Finally, numerous examples of the use of lithography simulation and its impact on the semiconductor industry are offered.

2. Optical Lithography Simulation

Optical lithography modeling began in the early 1970s when Rick Dill started an effort at IBM Yorktown Heights Research Center to describe the basic steps of the lithography process with mathematical equations. At a time when lithography was considered a true art, such an approach was met with much skepticism. The results of their pioneering work were published in a landmark series of papers in 1975 [1-4], now referred to as the "Dill papers." These papers not only gave birth to the field of lithography modeling, they represented the first serious attempt to describe lithography not as an art, but as a science. These papers presented a simple model for image formation with incoherent illumination, the first order kinetic "Dill model" of exposure, and an empirical model for development coupled with a cell algorithm for photoresist profile calculation. The Dill papers are still the most referenced works in the body of lithography literature.

While Dill's group worked on the beginnings of lithography simulation, a professor from the University of California at Berkeley, Andy Neureuther, spent a year on sabbatical working with Dill. Upon returning to Berkeley, Neureuther and another professor, Bill Oldham, started their own modeling effort. In 1979 they presented the first result of their effort, the lithography simulation program SAMPLE [5]. SAMPLE improved the state of the art in lithography modeling by adding partial coherence to the image calculations and by replacing the cell algorithm for dissolution calculations with a string algorithm. But more importantly, SAMPLE was made available to the lithography community. For the first time, researchers in the field could use modeling as a tool to help understand and improve their lithography processes.

Lithographic and Micromachining Techniques for Optical Component Fabrication, Ernst-Bernhard Kley, Hans Peter Herzig, Editors, Proceedings of SPIE Vol. 4440 (2001) © 2001 SPIE · 0277-786X/01/$15.00

The author began working in the area of lithographic simulation in 1983 and in 1985 introduced the model PROLITH (the Positive Resist Optical LITHography model) [6]. This model added an analytical expression for the standing wave intensity in the resist, a prebake model, a kinetic model for resist development (now known as the Mack model), and the first model for contact and proximity printing. PROLITH was also the first lithography simulator to run on a personal computer (the IBM PC), making lithography modeling accessible to all lithographers, from advanced researchers to process development engineers to manufacturing engineers. Over the years, this original, pre-commercial version of PROLITH advanced to include a model for contrast enhancement materials, the extended source method for partially coherent image calculations, and an advanced focus model for high numerical aperture imaging.

In 1990, a commercial version of PROLITH was introduced by FINLE Technologies and was called PROLITH/2, the second generation optical lithography model. In addition to PROLITH/2, PROXLITH/2 was developed to simulate contact and proximity printing, and PROLITH/3D extended the two-dimensional modeling of PROLITH/2 into three dimensions. Collectively, PROLITH/2 and PROLITH/3D are now referred to as PROLITH, the most widely used lithography simulator in the industry. In addition, the electron beam lithography simulator ProBEAM/3D, the electromagnetic field simulator ProMAX/2D, and the statistical CD error calculator ProCD have also been introduced by FINLE, now a division of KLA-Tencor.

PROLITH simulates the basic lithographic steps of image formation, resist exposure, post-exposure bake diffusion, and development to obtain a final resist profile. Figure 1 shows a basic schematic of the calculation steps required for lithography modeling. Below is a brief overview of the physical models found in PROLITH. More details on these models can be found in Ref. 7.

Aerial Image: The extended source method (also called the Abbe method) is used to predict the aerial image of a partially coherent diffraction limited or aberrated projection system based on scalar and/or vector diffraction theory. Single wavelength or broadband illumination can be used. Phase-shifting masks and off-axis illumination of arbitrary shape can be simulated. Pupil filters can be defined. The user can select a high numerical aperture scalar model to increase the accuracy of calculations for numerical apertures of 0.5 or greater, and a vector model can be used for very high numerical apertures. Arbitrarily complex two-dimensional mask features can be simulated (Figure 2a). The impact of synchronization errors during step and scan lithography are accounted for as a vibrational blurring of the image.

Standing Waves: An analytical expression is used to calculate the standing wave intensity as a function of depth into the resist, including the effects of resist bleaching, on planar substrates (Figure 2b). Film stacks can be defined below the resist with many layers between the resist and substrate. Contrast enhancement layers or top-layer anti-reflection coatings can also be included. The high numerical aperture models include the effects of non-vertical light propagation, and vector modeling is also included. For vector modeling, polarization and its effect on reflectivity is taken into account.

Prebake: Thermal decomposition of the photoresist photoactive compound during prebake is modeled using first order kinetics, resulting in a change in the resist's optical properties (the Dill parameters A and B). Solvent diffusion calculations describe the vertical distribution of solvent at the end of the prebake step. Many important bake effects, however, are not yet well understood and remain to be modeled.

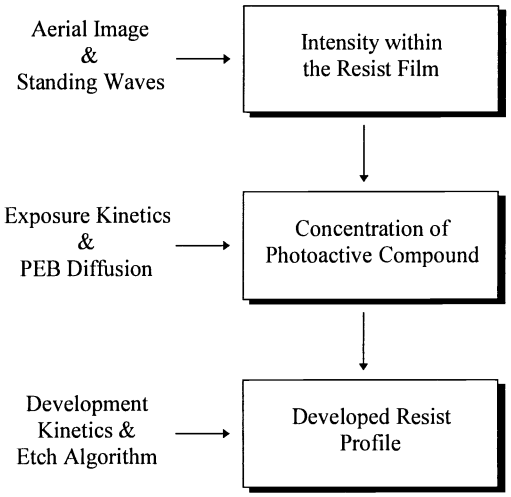

Figure 1a. Flow diagram of a basic optical lithography simulator.

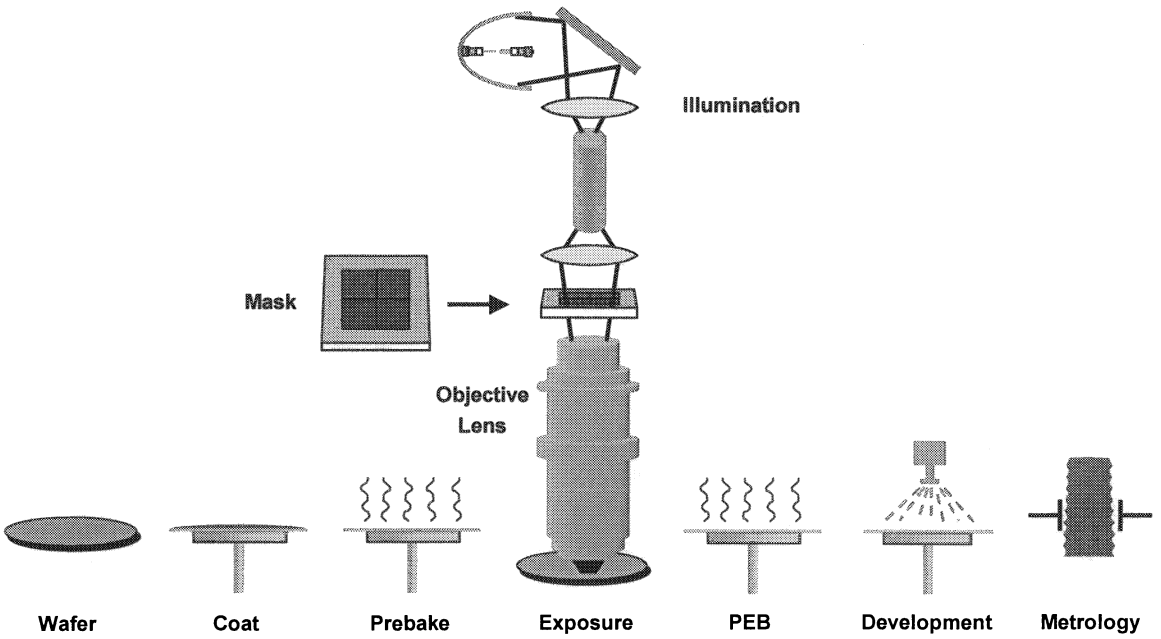

Figure 1b. Basic process steps simulated in optical lithography.

Exposure: First order kinetics are used to model the chemistry of exposure using the standard Dill ABC parameters [2], which can include the bleaching of the photoresist. Both positive and negative resists can be simulated.

Post-Exposure Bake: A three-dimensional diffusion calculation allows the post-exposure bake to reduce the effects of standing waves (Figure 2c). For chemically amplified resists, this diffusion is accompanied by an amplification reaction that accounts for crosslinking, blocking, or deblocking in an acid catalyzed reaction. Acid loss mechanisms and non-constant diffusivity can also be simulated using a three-dimensional reaction-diffusion algorithm and the Byers/Petersen model for chemically amplified resists [8, 9].

Development: One of several kinetic dissolution rate models is used in conjunction with the level set etching algorithm to determine the resist profile (Figure 2d). Surface inhibition or enhancement can also be taken into account. Alternatively, a data file of development rate information can be used.

CD Measurement: Multiple models for measurement of the photoresist linewidth give accuracy and flexibility to match the model to an actual CD measurement tool output. "Virtual" cross-sections of a three-dimensional simulated photoresist profile allow any type of metrology to be obtained.

The combination of the models described above provides a complete mathematical description of the optical lithography process. Use of the models allows the investigation of many interesting and important aspects of optical lithography.

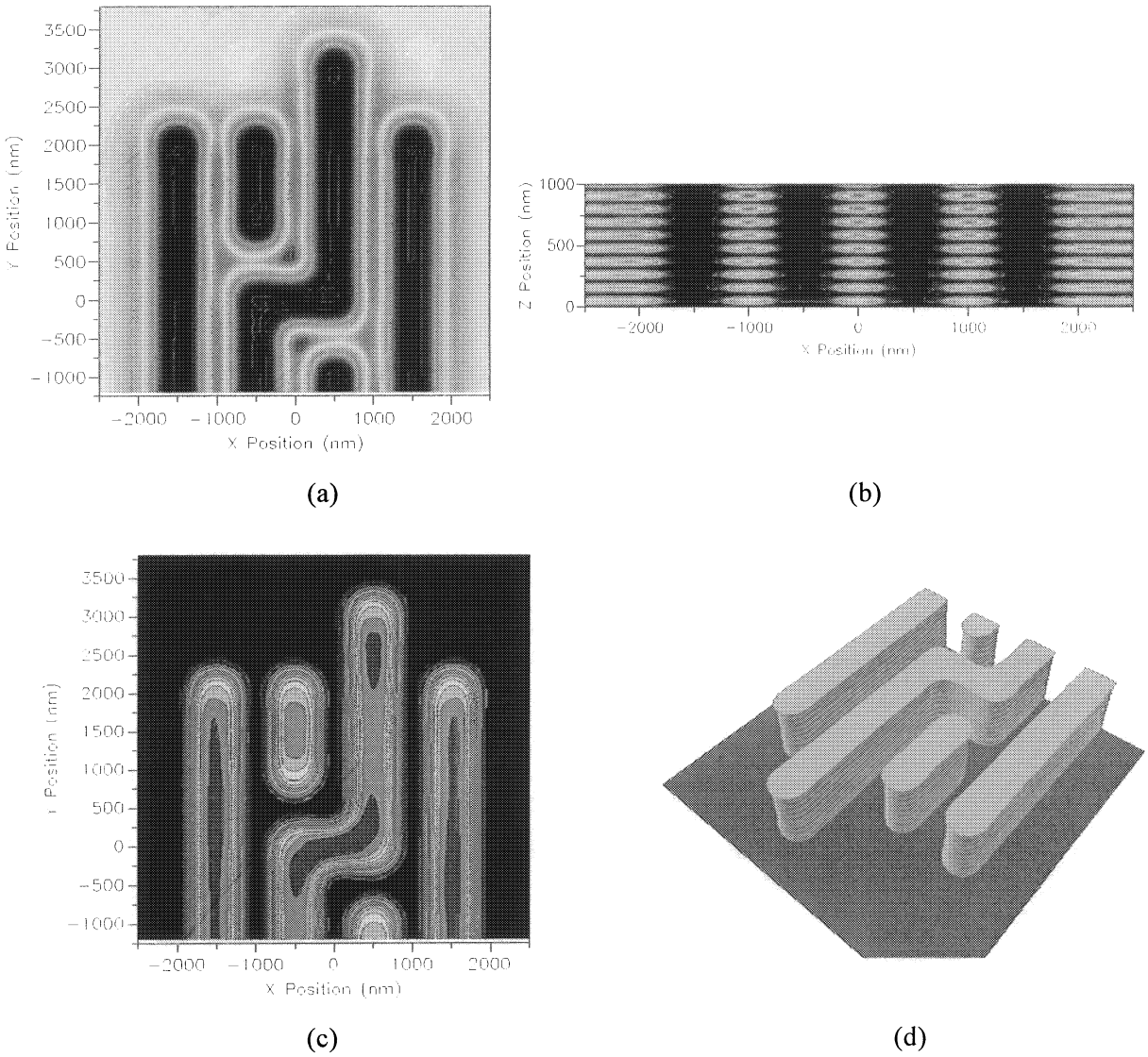

Figure 2. Simulation results for optical imaging of a typical logic pattern layout: (a) aerial image, (b) cross section of the image in resist showing standing waves, (c) latent image after exposure and post exposure bake, and (d) final resist profile.

3. Electron Beam Lithography Simulation

The general sequence of events required for electron beam lithography simulation is pictured in Figure 3. The Monte Carlo calculations use standard techniques. In particular, the method of Hawryluk, Hawryluk, and Smith [10] is followed. An electron scatters off nuclei in a pseudo-random fashion. The distance between collisions follows Poisson statistics using a mean free path based on the scattering cross-section of the nuclei. The energy loss due to a scattering event is calculated by the Beth energy loss formula. The "continuous slowing-down approximation" is used to spread this energy over the length traveled. Many electrons (typically 50,000 - 500,000) are used to bombard the material and an average energy deposited per electron as a function of radial position in the solid is determined. Some results of the Monte Carlo calculations are shown in Figures 4a and b.

The final result of the Monte Carlo calculation is the average energy distribution of a single electron of a given initial energy normally incident on the material/film stack at a single point. Electron beam exposure tools generate a spot or pixel of many electrons in a certain shape in order to expose the resist. For example, a typical e-beam exposure tool may use an electron beam that can be well approximated by a Gaussian-shaped spot of a certain full width at half maximum (FWHM). The Monte Carlo result can be used to generate a "pixel", the deposited energy for an average electron in the electron beam spot. The pixel is generated as the convolution of the Monte Carlo point energy distribution with the beam shape (Figure 4c).

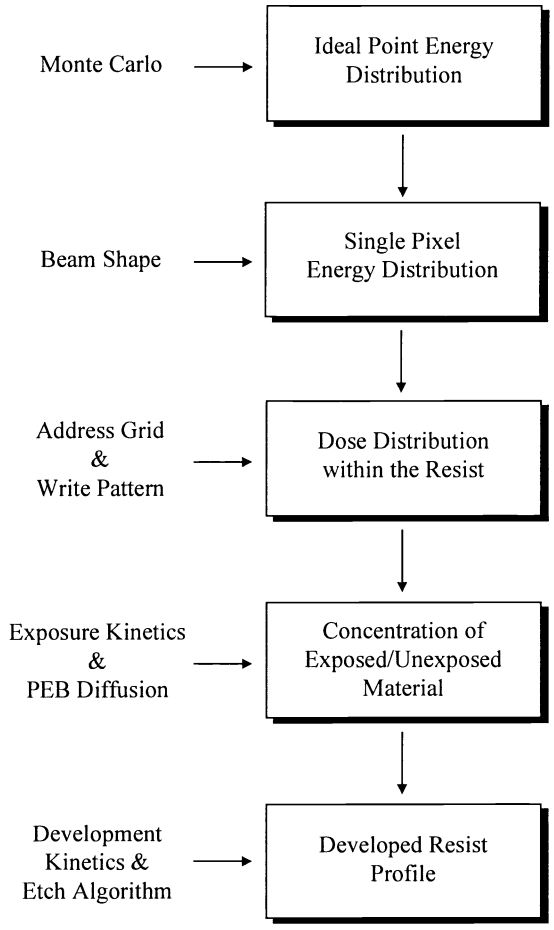

Figure 3. Flow diagram of a typical electron-beam lithography simulator.

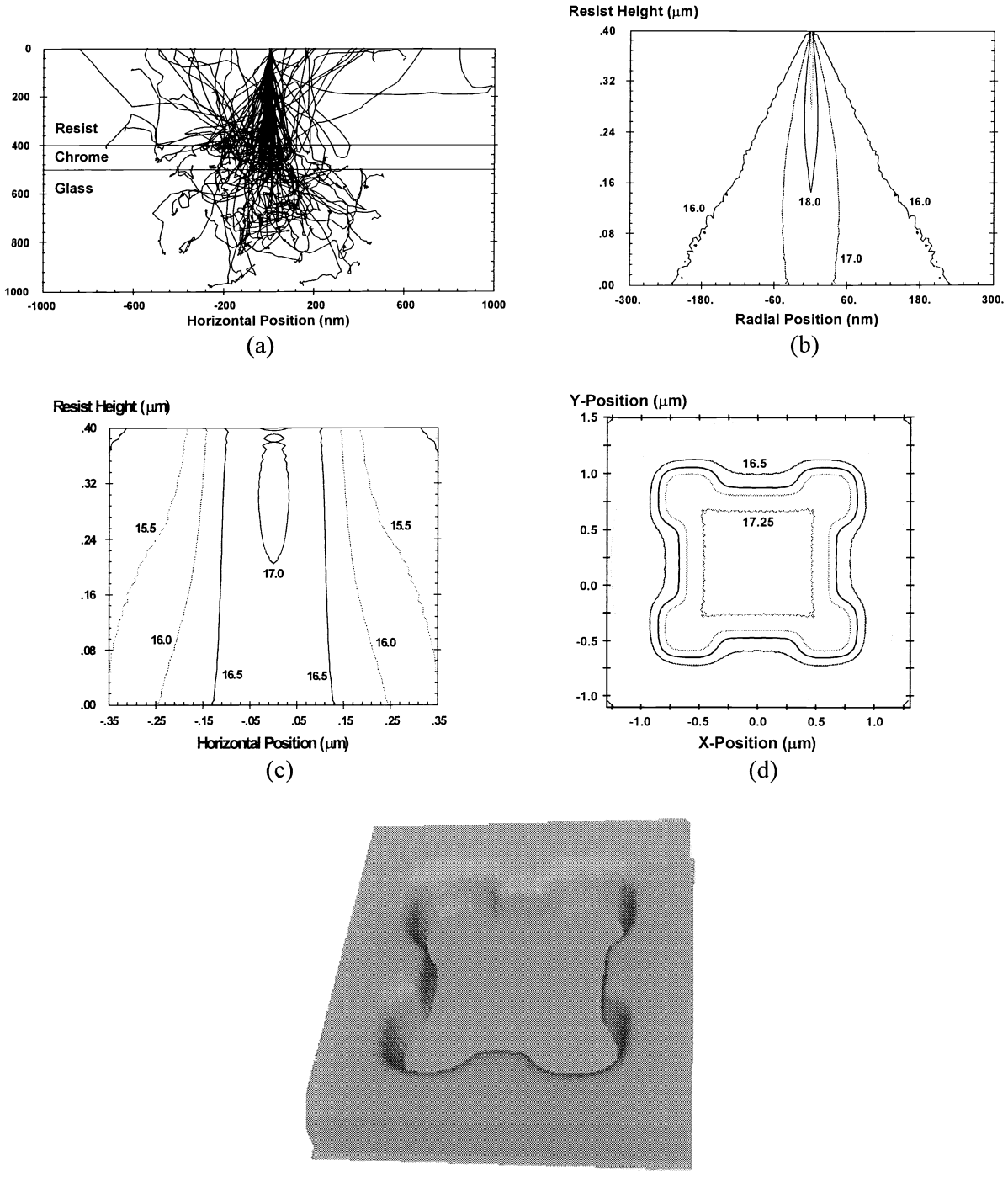

Figure 4. Simulation results for electron beam imaging in a 400nm resist film on 100nm of chrome on a glass substrate for an incident electron energy of 10KeV: (a) Monte Carlo trajectories, (b) Monte Carlo calculated energy deposited per electron, (c) pixel generation results for a 200nm (FWHM) Gaussian beam (contours show $\log_{10}(eV/cm^3/electron)$), (d) dose distributions for an address size of 100nm, at the bottom of the resist (contours show $\log_{10}(eV/cm^3)$), and (e) the three-dimensional resist profile of a 1.0μm contact with 0.4μm serifs.

The beam writing strategy used in an ebeam simulator should mimic the behavior of common electron beam lithography tools. A square address grid is defined with any grid size possible. Centered at each grid point is a beam pixel as described in the preceding paragraph. Each pixel address is assigned a dose (for example, in $\mu C/cm^2$), which essentially determines the number of electrons used in each pixel. The e-beam image is then the sum of the contributions from each pixel (Figure 4d). In the simplest scheme, pixels are either turned on or off to provide the desired pattern. Since each individual pixel can be controlled in dose, this writing strategy is very flexible. Proximity correction schemes and "gray-scale" exposure doses can easily be accommodated.

Resist exposure and development models have been borrowed from optical lithography simulation and applied to e-beam lithography. Full three-dimensional simulation can be performed by pulling together all of the components described above (Figure 4e).

4. Rigorous Electromagnetic Field Simulations

In general, optical lithography simulations use low numerical aperture approximations on the mask side of the imaging tool since most lithographic projection cameras use 4X or 5X reduction. Thus, a standard mask made of thin (100nm) chrome on a glass substrate would meet the basic criterion for the application of Kirchhoff's diffraction boundary conditions: dimensions in the plane of the mask are much bigger than the wavelength of light and dimensions in the direction of propagation of light are much smaller than the wavelength of light. Trends in lithography, however, are making these approximations less and less accurate. Resolution is being pushed to its limit of about half the wavelength of light. Thus, for a 4X mask, feature sizes on the mask are on the order of two wavelengths. More importantly, the use of strong phase shifting masks requires vertical topography on the mask of about one wavelength to create a 180 degree phase shift.

Alternating phase shifting masks made with a subtractive process result in phase shifted spaces where the phase shift results from etching a trench in the space of about one wavelength. The transmittance of light through such a narrow, deep trench is not well approximated by a simple shadow description of light transmittance. Full electromagnetic field (EMF) simulations are necessary to accurately describe the phase and amplitude transmittance properties of such masks [11]. Figure 5a shows a cross-section of a typical alternating phase shifting mask. Figure 5b shows the resulting electric field amplitude simulated for normally incident, E-polarized illumination at 248nm wavelength. Analysis of the near field diffraction pattern shows that the shifted space transmits only 89% as much light as the unshifted space, and with a 5 degree phase error for a mask that would be nominally correct in the Kirchhoff approximation.

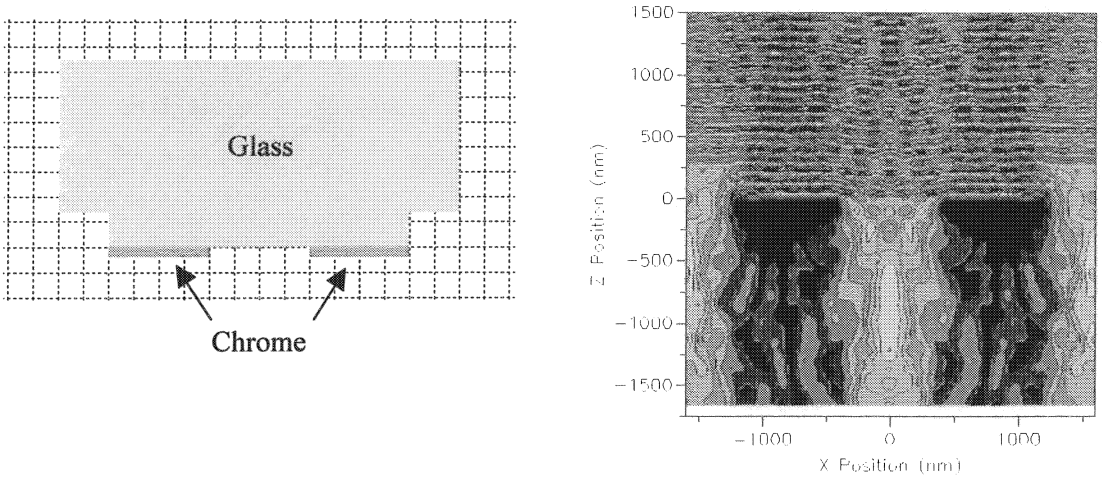

(a) (b)

Figure 5. Electromagnetic field simulations: (a) a typical alternating phase shifting mask, and (b) the resulting electric filed amplitude in and around the mask.

5. Statistical Modeling of Lithographic Errors

As the critical dimensions (CDs) of photolithographic processes continue to shrink, the processing of wafers becomes much more expensive and difficult. A result of these higher costs is the increased need to understand and control the CD distribution of lithography processes. Better control (i.e., reduction) of the CD distribution will lead to higher yields and more favorable bin sorting (speed distributions) of the final product. It is possible to accurately predict the parametric CD yield of a photolithographic process using well-established lithography modeling tools and the error convolution approach described below [12-15].

To predict the parametric CD yield of a photolithographic process using simulation, a simple three-step process is used. First, an analysis of the lithographic process must be performed to determine the error distributions of the input parameters. For example, it may be determined that exposure varies in a normal distribution with a mean at the nominal setting and a standard deviation of 5%. Second, a lithography simulator is used to create a multi-variable process response space (for example, final resist critical dimension versus focus, exposure, resist thickness, etc.). Third, by correlating the input error distribution with the process response space, a final CD distribution is generated. Analysis of the output distribution produces a predicted parametric CD yield using some acceptance criterion for CD. This number can be used to help optimize the yield of a given process.

Consider a simple example to illustrate the method – the effect of exposure errors on linewidth. The process response in this case is the well-known exposure latitude curve. If the input error distribution is known, correlation of the input error probability with the process response function gives the output error distribution. For this example let us assume that the exposure errors are normally distributed about the mean with a 3σ of 10% (Figure 6). Non-normal error sources can also be used, but a Gaussian error is used here for convenience.

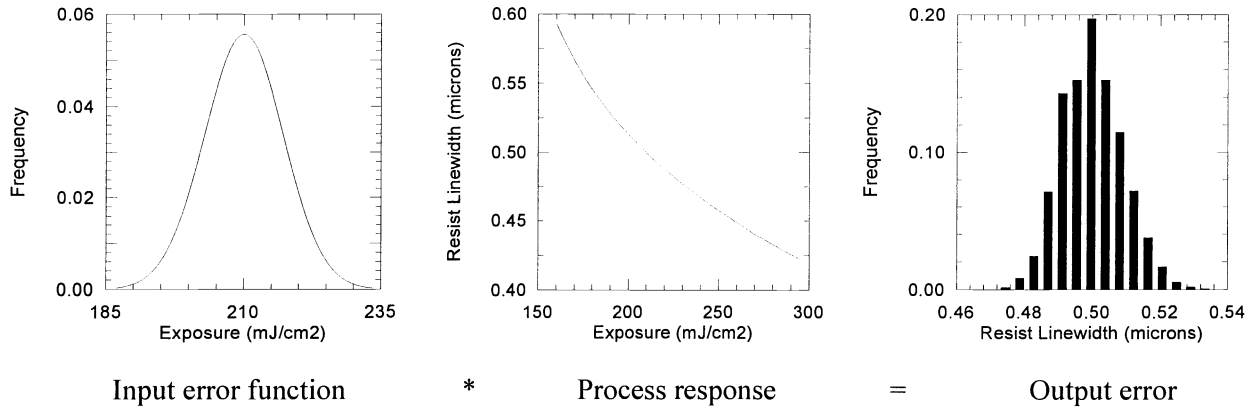

Figure 6. Resulting error distribution from a one-dimensional process response.

The error distribution is plotted as the frequency of occurrence (or probability of occurrence) versus exposure energy with arbitrary units for frequency. The process response is linewidth versus exposure energy. For any given exposure energy, there is a probability that this energy will occur (for example, 200 mJ/cm^2 has a probability of 0.021 in Figure 6). From the process response curve, an exposure energy corresponds to a specific CD (for example, 0.513 μm for an energy of 200 mJ/cm^2) and thus must have the probability of occurrence corresponding to the probability of the exposure energy. Correlation of the input error distribution with the process response results in a list of linewidth values with corresponding frequencies of occurrence. The linewidth can then be divided up into equal size bins (for Figure 6, the bin size is 0.004 μm) and all of the probabilities with CDs within a given bin are summed. The result is plotted as a histogram of frequency versus CD and represents the resulting output CD error distribution.

Figure 7 shows a typical example of the use of this type of statistical CD distribution prediction, comparing the simulation to an actual set of production CD data for a 0.6 micron i-line process [14].

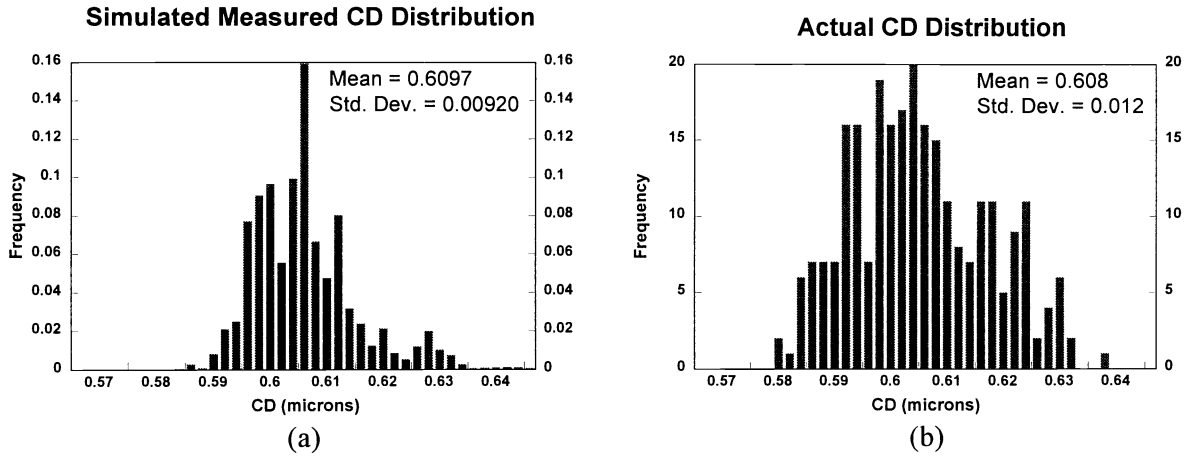

Figure 7. CD distributions for a 0.6 micron i-line process (a) simulated, and (b) actual data [14].

6. Uses of Lithography Simulation

In the twenty six years since optical lithography modeling was first introduced to the semiconductor industry, it has gone from a research curiosity to an indispensable tool for research, development, design and manufacturing. There are numerous examples of how modeling has had a dramatic impact on the evolution of lithography technology, and many more ways in which it has subtly, but undeniably, influenced the daily routines of lithography professionals. There are four major uses for lithography simulation: 1) as a research tool, performing experiments that would be difficult or impossible to do any other way, 2) as a development tool, quickly evaluating options, optimizing processes, or saving time and money by reducing the number of experiments in the fab, 3) as a manufacturing tool, for troubleshooting process problems and determining optimum process settings, and 4) as a learning tool, to help provide a fundamental understanding of all aspects of the lithography process. These four applications of lithography simulation are not distinct – there is much overlap among these basic categories.

6.1. Research Tool

Since the initial introduction of lithography simulation in 1975, modeling has had a major impact on research efforts in lithography. Here are some examples of how modeling has been used in research.

Modeling was used to suggest the use of dyed photoresist in the reduction of standing waves [16]. Experimental investigation into dyed resists didn't begin until 10 years later [17,18]. After phase-shifting masks were first introduced [19], modeling has proven to be indispensable in their study. Levenson used modeling extensively to understand the effects of phase masks [20]. One of the earliest studies of phase-shifting masks used modeling to calculate images for Levenson's original alternating phase mask, then showed how phase masks increased defect printability [21]. The same study used modeling to introduce the concept of the outrigger (or assist slot) phase mask. Since these early studies, modeling results have been presented in nearly every paper published on phase-shifting masks.

Off-axis illumination was first introduced as a technique for improving resolution and depth of focus based on modeling studies [22]. Since then, this technique has received widespread attention and has been the focus of many more simulation and experimental efforts. Using modeling, the advantages of having a variable numerical aperture, variable partial coherence stepper were discussed [22,23]. Since then, all major stepper vendors have offered variable NA, variable coherence systems. Modeling remains a critical tool for optimizing the settings of these flexible new machines. The use of pupil filters to enhance some aspects of lithographic performance has, to date, only been studied theoretically using lithographic models [24].

Modeling has been used in photoresist studies to understand the depth of focus loss when printing contacts in negative resists [25], the reason for artificially high values of resist contrast when surface inhibition is present [26], the potential for exposure optimization to maximize process latitude [27,28], and the role of diffusion in chemically amplified resists [29]. Lithographic models are now standard tools for photoresist design and evaluation.

Modeling has always been used as a tool for quantifying optical proximity effects and for defining algorithms for geometry dependent mask biasing [30,31]. Most people would consider modeling to be a required element of any optical proximity correction scheme. Defect printability has always been a difficult problem to understand. The printability of a defect depends considerably on the imaging system and resist used, as well as the position of the defect relative to other patterns on the mask and the size and transmission properties of the defect. Modeling has proven itself a valuable and accurate tool for predicting the printability of defects [32,33].

Modeling has also been used to understand metrology of lithographic structures [34-37] and continues to find new application in virtually every aspect of lithographic research. In fact, modeling has proven an indispensable tool for predicting future lithographic performance and evaluating the theoretical capabilities and limitations of extensions for optical lithography far into the future. One of the primary reasons that lithography modeling has become such a standard tool for research activities is the ability to simulate such a wide range of lithographic conditions. While laboratory experiments are limited to the equipment and materials on hand (a particular wavelength and numerical aperture of the stepper, a given photoresist), simulation gives an almost infinite array of possible conditions. From high numerical apertures to low wavelengths, hypothetical resists to arbitrary mask structures, simulation offers the ability to run "experiments" on steppers that you do not own with photoresists that have yet to be made. How else can one explore the shadowy boundary between the possible and the impossible?

6.2. Process Development Tool

Lithography modeling has also proven to be an invaluable tool for the development of new lithographic processes or equipment. Some of the more common uses include the optimization of dye loadings in photoresist [38,39], simulation of substrate reflectivity [40,41], the applicability and optimization of top and bottom antireflection coatings [42,43] and underlying film stacks, and simulation of the effect of bandwidth on swing curve amplitude [44,45]. In addition, simulation has been used to help understand the use of thick resists for thin film head manufacture [46] as well as other non-semiconductor applications.

Modeling is used extensively by makers of photoresist to evaluate new formulations [47,48] and to determine adequate measures of photoresist performance for quality control purposes [49]. Resist users often employ modeling as an aid for new resist evaluations. On the exposure tool side, modeling has become an indispensable part of the optimization of the numerical aperture and partial coherence of a stepper [50-52] and in the understanding of the print bias between dense and isolated lines [53]. The use of optical proximity correction software requires rules on how to perform the corrections, which are often generated with the help of lithography simulation [54].

As a development tool, lithography simulation excels due to its speed and cost-effectiveness. Process development usually involves running numerous experiments to determine optimum process conditions, shake out possible problems, determine sensitivity to variables, and write specification limits on the inputs and outputs of the process. These activities tend to be both time consuming and costly. Modeling offers a way to supplement laboratory experiments with simulation experiments to speed up this process and reduce costs. Considering that a single experimental run in a wafer fabrication facility can take from hours to days, the speed advantage of simulation is considerable. This allows a greater number of simulations than would be practical (or even possible) in the fab.

6.3. Manufacturing Tool

Although there is less published material on the use of lithography simulation in manufacturing environments [55-57], the reason is the limited publications by people in manufacturing rather than the limited use of lithography modeling. The use of simulation in a manufacturing environment has three primary goals: to reduce the number of test or experimental wafers which must be run through the production line, to troubleshoot problems in the fab, and to aid in decision making by providing facts to support engineering judgment and intuition.

Running test wafers through a manufacturing line is costly not so much due to the cost of the test, but due to the opportunity cost of not running product [58]. If simulation can reduce the time a manufacturing line is not running product even slightly, the return on investment can be significant. Simulation can also aid in the time required to bring a new process on-line and in the establishment of the base-line capability of a new process.

6.4. Learning Tool

Although the research, development and manufacturing applications of lithography simulation presented above give ample benefits of modeling based on time, cost and capability, the underlying power of simulation is its ability to act as a learning tool. Proper application of modeling allows the user to learn efficiently and effectively. There are many reasons why this is true. First, the speed of simulation versus experimentation makes feedback much more timely. Since learning is a cycle (an idea, an experiment, a measurement, then comparison back to the original idea), faster feedback allows for more cycles of learning. Since simulation is very inexpensive, there are fewer inhibitions and more opportunities to explore ideas. And, as the research application has shown us, there are fewer physical constraints on what "experiments" can be performed. Further, simulation allows the user to probe the otherwise inaccessible intermediate steps of aerial images and latent images and separate out the effects of multiple interacting variables.

7. Conclusions

The impact of simulation on optical lithography has been undeniably dramatic. However, the best is yet to come. The continuing improvement in models, software, and measured input parameters results in greater use of simulation almost on a daily basis. Like a lithography calculator, lithography simulation is becoming a commonplace tool that engineers rely on to do their jobs.

8. References

1. F. H. Dill, "Optical Lithography," *IEEE Trans. Electron Devices*, ED-22, No. 7 (1975) pp. 440-444.
2. F. H. Dill, W. P. Hornberger, P. S. Hauge, and J. M. Shaw, "Characterization of Positive Photoresist," *IEEE Trans. Electron Devices*, ED-22, No. 7 (July, 1975) pp. 445-452.
3. K. L. Konnerth and F. H. Dill, "In-Situ Measurement of Dielectric Thickness During Etching or Developing Processes," *IEEE Trans. Electron Devices*, ED-22, No. 7 (1975) pp. 452-456.
4. F. H. Dill, A. R. Neureuther, J. A. Tuttle, and E. J. Walker "Modeling Projection Printing of Positive Photoresists," *IEEE Trans. Electron Devices*, ED-22, No. 7 (1975) pp. 456-464.
5. W. G. Oldham, S. N. Nandgaonkar, A. R. Neureuther and M. O'Toole, "A General Simulator for VLSI Lithography and Etching Processes: Part I - Application to Projection Lithography," *IEEE Trans. Electron Devices*, ED-26, No. 4 (April, 1979) pp. 717-722.
6. C. A. Mack, "PROLITH: A Comprehensive Optical Lithography Model," *Optical Microlithography IV, Proc.*, SPIE Vol. 538 (1985) pp. 207-220.
7. C. A. Mack, Inside PROLITH: A Comprehensive Guide to Optical Lithography Simulation, FINLE Technologies (Austin, TX: 1997).
8. J. Byers, J. Petersen, and J. Sturtevant, "Calibration of Chemically Amplified Resist Models," *Advances in Resist Technology and Processing XIII, Proc.*, SPIE Vol. 2724 (1996) pp. 156-162.
9. J. Petersen and J. Byers, "Examination of Isolated and Grouped Feature Bias in Positive Acting, Chemically Amplified Resist Systems," *Advances in Resist Technology and Processing XIII, Proc.*, SPIE Vol. 2724 (1996) pp. 163-171.
10. R. J. Hawryluk, A. M. Hawryluk, and H. I. Smith, "Energy Dissipation in a Thin Polymer Film by Electron Beam Scattering," *Journal of Applied Physics*, Vol. 45, No. 6 (June, 1974) pp. 2551-2566.
11. R. L Gordon, C. A. Mack, and J. S. Petersen, "Designing Manufacturable Alternating Phase Shifting Masks for Unpolarized Illumination, *SPIE Proceedings* Vol. 3873 (1999) p. 97.
12. C.A. Mack and E.W. Charrier, "Yield Modeling for Photolithography", *OCG Interface '94* (1994), pp. 171-182.
13. E.W. Charrier and C.A. Mack, "Yield Modeling and Enhancement for Optical Lithography," *Optical/Laser Microlithography VIII*, Proc., SPIE Vol. 2440 (1995), pp 435-447.
14. E. W. Charrier, C.J. Progler, C.A. Mack, "Comparison of Simulated and Experimental CD-Limited Yield for a Submicron i-Line Process", *Microelectronic Manufacturing, Yield, Reliability and Failure Analysis,* Proc. SPIE Vol 2635, (1995), pp. 84-94.
15. E.W. Charrier, C.A. Mack, Q. Zuo, M. Maslow, "Methodology for Utilizing CD Distributions for Optimization of Lithographic Processes," *Optical Microlithography X*, Proc., SPIE (1997).

16. A. R. Neureuther and F. H. Dill, "Photoresist Modeling and Device Fabrication Applications," Optical And Acoustical Micro-Electronics, Polytechnic Press (New York: 1974) pp. 233-249.
17. H. L. Stover, M. Nagler, I. Bol, and V. Miller, "Submicron Optical Lithography: I-line Lens and Photoresist Technology," *Optical Microlith. III*, Proc., SPIE Vol. 470 (1984) pp. 22-33.
18. I. I. Bol, "High-Resolution Optical Lithography using Dyed Single-Layer Resist," *Kodak Microelec. Seminar Interface '84* (1984) pp. 19-22.
19. M. D. Levenson, N. S. Viswanathan, R. A. Simpson, "Improving Resolution in Photolithography with a Phase-Shifting Mask," *IEEE Trans. Electron Devices*, Vol. ED-29, No. 12 (Dec. 1982) pp. 1828-1836.
20. M. D. Levenson, D. S. Goodman, S. Lindsey, P. W. Bayer, and H. A. E. Santini, "The Phase-Shifting Mask II: Imaging Simulations and Submicrometer Resist Exposures," *IEEE Trans. Electron Devices*, Vol. ED-31, No. 6 (June 1984) pp. 753-763.
21. M. D. Prouty and A. R. Neureuther, "Optical Imaging with Phase Shift Masks," *Optical Microlith. III*, Proc., SPIE Vol. 470 (1984) pp. 228-232.
22. C. A. Mack, "Optimum Stepper Performance Through Image Manipulation," *KTI Micro-electronics Seminar, Proc.*, (1989) pp. 209-215.
23. C. A. Mack, "Algorithm for Optimizing Stepper Performance Through Image Manipulation," *Optical/Laser Microlithography III, Proc.*, SPIE Vol. 1264 (1990) pp. 71-82.
24. H. Fukuda, T. Terasawa, and S. Okazaki, "Spatial Filtering for Depth-of-focus and Resolution Enhancement in Optical Lithography," *Journal of Vacuum Science and Technology*, Vol. B9, No. 6 (Nov/Dec 1991) pp. 3113-3116.
25. C. A. Mack and J. E. Connors, "Fundamental Differences Between Positive and Negative Tone Imaging," *Optical/Laser Microlithography V, Proc.*, SPIE Vol. 1674 (1992) pp. 328-338, and *Microlithography World*, Vol. 1, No. 3 (Jul/Aug 1992) pp. 17-22.
26. C. A. Mack, "Lithographic Optimization Using Photoresist Contrast," *KTI Microlithography Seminar, Proc.*, (1990) pp. 1-12, and *Microelectronics Manufacturing Technology*, Vol. 14, No. 1 (Jan. 1991) pp. 36-42.
27. C. A. Mack, "Photoresist Process Optimization," *KTI Microelectronics Seminar, Proc.*, (1987) pp. 153-167.
28. P. Trefonas and C. A. Mack, "Exposure Dose Optimization for a Positive Resist Containing Poly-functional Photoactive Compound," *Advances in Resist Technology and Processing VIII, Proc.*, SPIE Vol. 1466 (1991).
29. J. S. Petersen, C. A. Mack, J. Sturtevant, J. D. Byers and D. A. Miller, "Non-constant Diffusion Coefficients: Short Description of Modeling and Comparison to Experimental Results," *Advances in Resist Technology and Processing XII, Proc.*, SPIE Vol. 2438 (1995).
30. C. A. Mack and P. M. Kaufman, "Mask Bias in Submicron Optical Lithography," *Jour. Vac. Sci. Tech.*, Vol. B6, No. 6 (Nov./Dec. 1988) pp. 2213-2220.
31. N. Shamma, F. Sporon-Fielder and E. Lin, "A Method for Correction of Proximity Effect in Optical Projection Lithography," *KTI Microelectronics Seminar, Proc.*, (1991) pp. 145-156.
32. A. R. Neureuther, P. Flanner III, and S. Shen, "Coherence of Defect Interactions with Features in Optical Imaging," *Jour. Vac. Sci. Tech.*, Vol. B5, No. 1 (Jan./Feb. 1987) pp. 308-312.
33. J. Wiley, "Effect of Stepper Resolution on the Printability of Submicron 5x Reticle Defects," *Optical/Laser Microlithography II, Proc.*, SPIE Vol. 1088 (1989) pp. 58-73.
34. L.M. Milner, K.C. Hickman, S.M. Gasper, K.P. Bishop, S.S.H. Naqvi, J.R. McNeil, M. Blain, and B.L. Draper, "Latent Image Exposure Monitor Using Scatterometry," SPIE Vol. 1673 (1992) pp. 274-283.
35. K.P. Bishop, L.M. Milner, S.S.H. Naqvi, J.R. McNeil, and B.L. Draper, "Use of Scatterometry for Resist Process Control," SPIE Vol. 1673 (1992) pp. 441-452
36. L.M. Milner, K.P. Bishop, S.S.H. Naqvi, and J.R. McNeil, "Lithography Process Monitor Using Light Diffracted from a Latent Image," SPIE Vol. 1926 (1993) pp. 94-105.
37. S. Zaidi, S.L. Prins, J.R. McNeil, and S.S.H. Naqvi, "Metrology Sensors for Advanced Resists," SPIE Vol. 2196 (1994) pp. 341-351
38. J.R. Johnson, G.J. Stagaman, J.C. Sardella, C.R. Spinner III, F. Liou, P. Tiefonas, and C. Meister, "The Effects of Absorptive Dye Loading and Substrate Reflectivity on a 0.5 μm I-line Photoresist Process," SPIE Vol. 1925 (1993) pp. 552-563.
39. W. Conley, R. Akkapeddi, J. Fahey, G. Hefferon, S. Holmes, G. Spinillo, J. Turtevant, and K. Welsh, "Improved Reflectivity Control of APEX-E Positive Tone Deep-UV Photoresist," SPIE Vol. 2195 (1994) pp. 461-476.

40. N. Thane, C. Mack, and S. Sethi, "Lithographic Effects of Metal Reflectivity Variations," SPIE Vol. 1926 (1993) pp. 483-494.
41. B. Singh, S. Ramaswami, W. Lin, and N. Avadhany, "IC Wafer Reflectivity Measurement in the UV and DUV and Its Application for ARC Characterization," SPIE Vol. 1926 (1993) pp. 151-163.
42. S.S. Miura, C.F. Lyons, and T.A. Brunner, "Reduction of Linewidth Variation over Reflective Topography," SPIE Vol. 1674 (1992) pp. 147-156.
43. H. Yoshino, T. Ohfuji, and N. Aizaki, "Process Window Analysis of the ARC and TAR Systems for Quarter Micron Optical Lithography," SPIE Vol. 2195 (1994) pp. 236-245.
44. G. Flores, W. Flack, and L. Dwyer, "Lithographic Performance of a New Generation I-line Optical System: A Comparative Analysis," SPIE Vol. 1927 (1993) pp. 899-913.
45. B. Kuyel, M. Barrick, A. Hong, and J. Vigil, "0.5 Micron Deep UV Lithography Using a Micrascan-90 Step-And-Scan Exposure Tool," SPIE Vol. 1463 (1991) pp. 646-665.
46. G.E. Flores, W.W. Flack, and E. Tai, "An Investigation of the Properties of Thick Photoresist Films," SPIE Vol. 2195 (1994) pp. 734-751.
47. H. Iwasaki, T. Itani, M. Fujimoto, and K. Kasama, "Acid Size Effect of Chemically Amplified Negative Resist on Lithographic Performance," SPIE Vol. 2195 (1994) pp. 164-172.
48. U. Schaedeli, N. Münzel, H. Holzwarth, S.G. Slater, and O. Nalamasu, "Relationship Between Physical Properties and Lithographic Behavior in a High Resolution Positive Tone Deep-UV Resist," SPIE Vol. 2195 (1994) pp. 98-110.
49. K. Schlicht, P. Scialdone, P. Spragg, S.G. Hansen, R.J. Hurditch, M.A. Toukhy, and D.J. Brzozowy, "Reliability of Photospeed and Related Measures of Resist Performances," SPIE Vol. 2195 (1994) pp. 624-639.
50. R.A. Cirelli, E.L. Raab, R.L. Kostelak, and S. Vaidya, "Optimizing Numerical Aperture and Partial Coherence to Reduce Proximity Effect in Deep-UV Lithography," SPIE Vol. 2197 (1994) pp. 429-439.
51. B. Katz, T. Rogoff, J. Foster, B. Rericha, B. Rolfson, R. Holscher, C. Sager, and P. Reynolds, "Lithographic Performance at Sub-300 nm Design Rules Using High NA I-line Stepper with Optimized NA and σ in Conjunction with Advanced PSM Technology," SPIE Vol. 2197 (1994) pp. 421-428.
52. P. Luehrmann, and S. Wittekoek, "Practical 0.35 μm I-line Lithography," SPIE Vol. 2197 (1994) pp. 412-420.
53. V.A. Deshpande, K.L. Holland, and A. Hong, "Isolated-grouped Linewidth Bias on SVGL Micrascan," SPIE Vol. 1927 (1993) pp. 333-352.
54. R.C. Henderson, and O.W. Otto, "Correcting for Proximity Effect Widens Process Latitude," SPIE Vol. 2197 (1994) pp. 361-370.
55. H. Engstrom and J. Beacham, "Online Photolithography Modeling Using Spectrophotometry and PROLITH/2," SPIE Vol. 2196 (1994) pp. 479-485.
56. J. Kasahara, M. V. Dusa, and T. Perera, "Evaluation of a Photoresist Process for 0.75 Micron, G-line Lithography," SPIE Vol. 1463 (1991) pp. 492-503.
57. E. A. Puttlitz, J. P. Collins, T. M. Glynn, L. L. Linehan, "Characterization of Profile Dependency on Nitride Substrate Thickness for a Chemically Amplified I-line Negative Resist," SPIE Vol. 2438 (1995) pp. 571-582.
58. P. M. Mahoney and C. A. Mack, "Cost Analysis of Lithographic Characterization: An Overview," *Optical/Laser Microlithography VI, Proc.*, SPIE Vol. 1927 (1993) pp. 827-832.